

NOVEL ELECTROCHEMICAL REACTIONS RELATED TO ELECTRODEPOSITION AND ELECTROCHEMICAL SYNTHESIS

Y. Ito and T. Nishikiori

Department of Fundamental Energy Science, Graduate School of Energy Science,
Kyoto University, Sakyo-ku, Kyoto 606-8501, Japan
(E-mail: y-ito@energy.kyoto-u.ac.jp)

(Received 4 January 2003; accepted 16 February 2003)

Abstract

Novel electrochemical reactions in molten salts related to electrodeposition and electrochemical synthesis are reviewed to show their usefulness and possibilities in producing functional materials. Surface nitriding of various metals and stainless steels is possible by the use of anodic reaction of nitride ion (N^{3-}) in LiCl-KCl-Li₃N melts. Electrochemical hydrogen absorption/desorption reaction occurs in molten salts containing hydride ion (H). Electrochemical implantation and displantation can be applied to form transition metal-rare earth metal alloys in LiCl-KCl melts containing rare earth chlorides. As non-conventional electrochemical reactions, direct electrochemical reduction of SiO₂ to Si, discharge electrolysis to form metal oxide particles and electrochemical plantation of Zr on ceramics are described.

Keywords: molten salt, electrodeposition and electrochemical synthesis, metal nitride, metal hydride, transition metal-rare earth metal alloy, direct reduction of SiO₂

1. Introduction

Standing at the threshold of the 21st century, we must strive toward sustainable economic growth while maintaining environmental protections. Recent technological developments have focused on high functionalization of materials, achieving low environmental impact as well as low manufacturing cost. Moreover, the development of

recycling processes is expected to include extra steps to add further functions to the recycled resources, and furthermore, the function-adding methods must have both good flexibility and environmental compatibility. When considering the functionalization of materials, for example, mesoscopic pore formation, fine particle formation, alloying or addition of various elements and surface modification are promising. Currently, these types of functionalization can be conducted by means of sol-gel methods, physical or chemical vapor deposition, mechanical alloying, ion-implantation, electrochemical methods and others. Among them, the electrochemical method may come to play important roles due to its low environmental impact, low energy consumption and good flexibility. The authors and co-workers have identified the advantageous characteristics of the electrochemical method and studied electrochemical reactions in molten salts to obtain highly functionalized materials.

Electrochemical technology using molten salts has been most famously applied to aluminum electrolysis [1-3], production of highly reactive metals [4-5] and electroplating of refractory metals [6-8]. Molten salts are, in general, chemically and physically stable, highly electrically conductive, and in many cases, they dissolve various chemical species with sufficiently high concentration. Moreover, they have wide electrochemical windows; for example, in the case of alkali halides, the accessible potential range is as wide as between alkali metal deposition (cathodic limit) and halogen gas evolution (anodic limit). Recently, the authors and co-workers have found attractive, feasible ways to obtain various kinds of highly functionalized materials by utilizing electrochemical reactions in molten salts. This review article describes investigations of selected novel reactions performed in our laboratory, which are related to electrodeposition and electrochemical synthesis of highly functionalized materials.

2. Surface nitriding of metals

Metal nitrides have been paid considerable attention in recent years as high hardness and wear resistant/corrosion resistant (*Ti-N*, *Zr-N*, *Cr-N*), magnetic (*Sm-Fe-N*, *Fe-N*), semiconductor (*Ga-N*, *Al-N*), battery (*Co-Li-N*) etc materials.

The authors and co-workers have proposed a novel surface nitriding technique by utilizing a simple electrochemical reaction in alkali metal halide melts containing nitride ion (N^{3-}). This technique is conducted by the anodic oxidation of N^{3-} on a metal (M – metals and alloys) electrode according to the following consecutive reactions:



where anodically-produced adsorbed nitrogen atoms react with the outermost metal surface and diffuse towards the bulk, from which the nitrogen concentration gradient is usually observed in the formed nitride layer. It is noteworthy that there is a possibility for this process to precisely and easily control structural characteristics of surface nitride

layer (composition, surface texture, morphology, thickness etc.) by controlling electrolysis potential and time. This electrochemical surface nitriding has been confirmed so far for various metal-nitrogen systems including *Ti-N* [9-11], *Zr-N* [12], *Fe-N* [13], *Al-N* [14], *Co-N* [15], *Cr-N* [16], *Ga-N* [17], *Sm-Fe-N* [18] and *C-N* [19].

Since its birth, nitriding has been used principally for steels to improve their surface hardness and tribological properties. Most recently, the authors and co-workers have succeeded in the electrochemical surface nitriding of the SUS430 ferritic stainless steel (*Fe-18 wt% Cr*) [20]. Fig. 1 shows cross-sectional SEM image and microhardness profile after potentiostatic electrolysis at 1.0 V (vs. *Li⁺/Li*) for 10 hours at 773K.

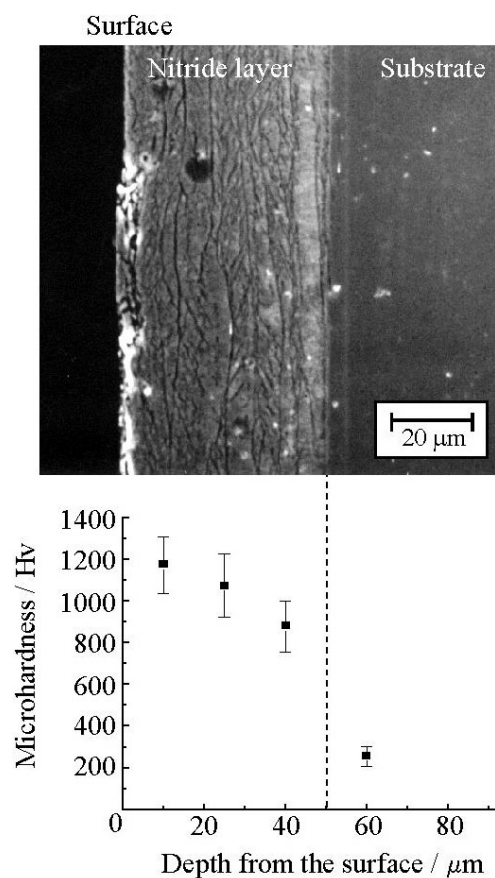


Figure 1. Cross-sectional SEM image and microhardness profile of the SUS430 stainless steel specimen after potentiostatic electrolysis at 1.0 V for 10 hours in *LiCl-KCl* melts containing 1.0 mol. % *Li₃N* at 723 K.

An adhesive coherent layer is formed on the surface. Surface analyses by XRD and XPS certified that the surface layer contains CrN precipitates in the $\alpha-Fe$ matrix. The hardness in the nitride layer increases up to about 1000 Hv, which is reasonable with reference to those nitride layers obtained by other nitriding processes. Fig. 2 shows the growth of the nitride layer at different applied potentials (0.5 V, 1.0 V and 1.5 V). In all cases, the growth kinetics follows parabolic rate law, which implies that the electrochemical nitriding is controlled by a diffusion process. Furthermore, it is noticed that the growth rate strongly depends on the applied potential. This result indicates that the chemical potential of anodically formed adsorbed nitrogen, which directly affects the nitride growth, is controlled by the applied potential.

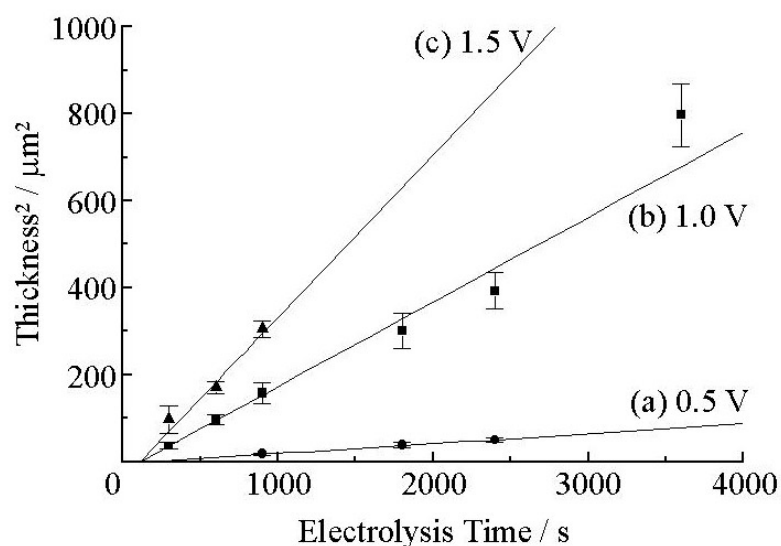


Figure 2. Square of the thickness of the nitride layer as a function of electrolysis time for different applied potentials: (a) 0.5 V, (b) 1.0 V and (c) 1.5 V.

When considering practical application of this process, it has the drawback of using expensive N^{3-} source (Li_3N) and the accumulation of excessive lithium cation. However, these would be overcome since nitrogen gas can be cathodically reduced to N^{3-} by using a gas electrode [21]:



Using this cathode reaction as an inexpensive N^{3-} source, a new nitriding system is proposed whose principle is shown in Fig. 3. The possibility of this process using N_2 gas cathode has been verified by the experiment of continuous nitriding of titanium [21].

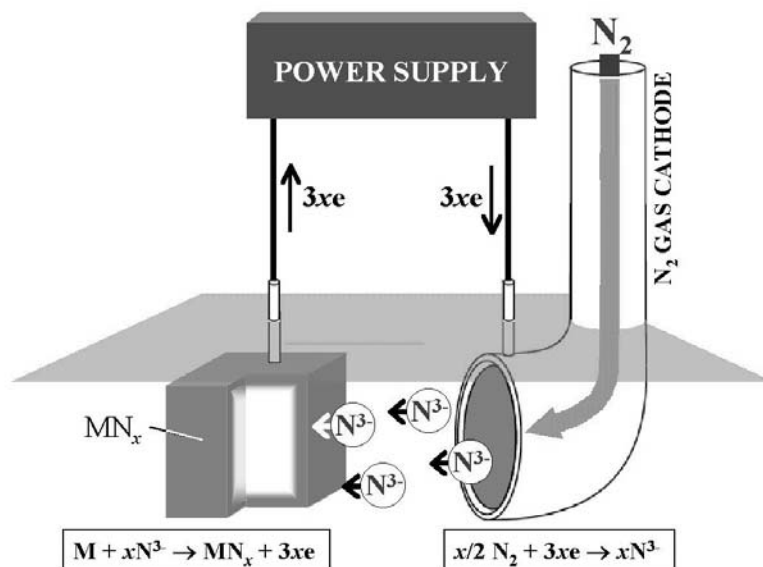


Figure 3. Schematic illustration of the electrochemical surface nitriding of metals in molten salts. In this method, nitride ion (N^{3-}) produced by the reduction from nitrogen gas at the cathode is anodically oxidized and reacts with metal surface to produce nitride layer with N concentration gradient.

3. Hydrogen absorbing/desorbing reactions

3.1. Investigations of metal hydrides

If one finds suitable materials that absorb much hydrogen even at high temperature, it will be possible to use them for various engineering applications, for instance, materials for hydrogen storage or transportation in hydrogen energy system, metal membranes for hydrogen purification, hydrogen sensors and target metal hydrides for neutron generator. On the other hand, if one finds suitable coating materials that prevent hydrogen permeation, it will become possible to apply them to the structural materials in hydrogen atmosphere to prevent hydrogen embrittlement. Taking into consideration these possibilities, the authors and co-workers have been investigating the electrochemical reactions of $M-H/H^-$ systems. It provides us with precise and useful information on hydrogen absorbing/desorbing and/or hydrogen permeation characteristics of various metals, alloys and compounds at high temperatures.

In the case of the *Ti-H* system, the thermodynamic and kinetic properties have been investigated precisely in the *LiCl-KCl-LiH* and *LiBr-KBr-CsBr-LiH* melts at 523-773 K [22-25]. For the thermodynamic investigation, galvanostatic electrolysis was conducted on titanium electrode intermittently to absorb hydrogen according to the following reaction,



and stable open-circuit potentials were measured. Since the hydrogen contents (x in TiH_x) were estimated by assuming 100% current efficiency [22], electrode potential–composition–temperature (*E-C-T*) relationships were obtained as shown in Fig. 4. From these relationships, the thermodynamic quantities of all phase states of TiH_x were evaluated, which are well consistent with those reported by other authors using conventional thermochemical methods [22, 24]. On the other hand, for the kinetic investigations, the diffusion coefficients of hydrogen in TiH_x with various hydrogen contents were estimated by chronopotentiometry, potential-step chronoamperometry and AC impedance spectroscopy [25]. The obtained values are in agreement with reported values. It was also found that the hydrogen diffusion behavior is strongly affected by the phase transformations.

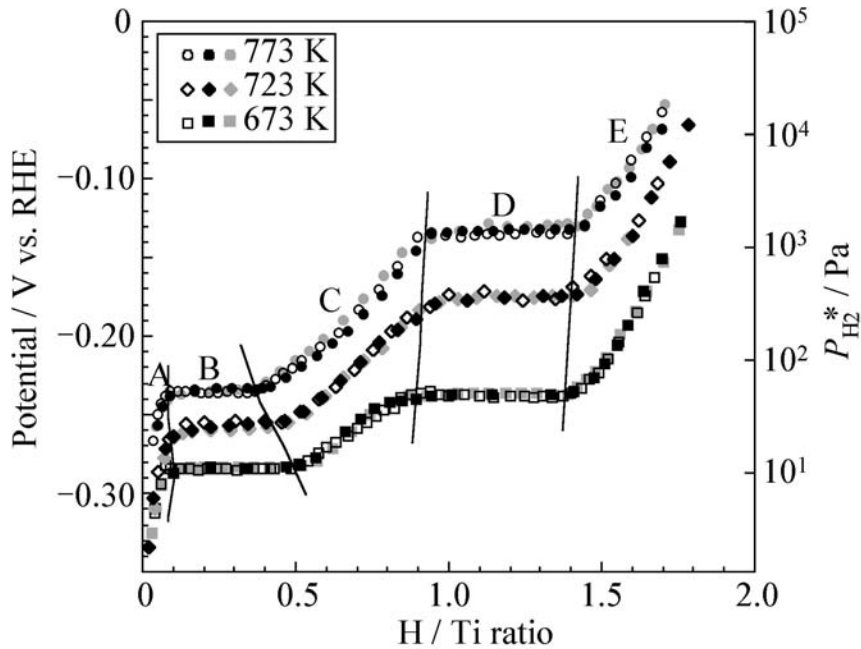


Figure 4. Electrode potential-composition-temperature (*E-C-T*) relationships in the (A) α , (C) β , (E) δ single-phase regions, and (B) $\alpha+\beta$, (D) $\beta+\delta$ co-existing phase regions of the *Ti-H* system at 673, 723 and 773 K.

*Equivalent hydrogen pressure is calculated at 723 K.

The electrochemical hydrogen absorbing/desorbing behavior of *Pd* and *Pd-Li* alloys with various lithium contents was also investigated by a similar method. The results showed that hydrogen-absorbing properties are significantly larger for electrodes with higher lithium concentration. These characteristics for *Pd-Li* alloys might be explained by stronger interaction of *Li-H* than of *Pd-H* [26].

The authors confirm that this electrochemical technique has many advantages, such as operability, safety and accuracy in comparison with conventional methods using hydrogen gas. So far, that method is considered to be applicable in the hydrogen pressure range up to 1 atm and in the temperature range from about 500 K to 800 K. Under these conditions, this method has a potential to be established as a general method for investigating thermodynamic and kinetic properties of various *M-H* systems.

3.2. Hydrogen impermeable coatings

As one of the application examples of the above electrochemical technique, hydrogen permeability was investigated for TiN_x films prepared by electrochemical method described in section 2 and by other conventional methods [27-28]. It is quite interesting to note that a very thin TiN_x layer formed on titanium substrate decreases the hydrogen absorption/desorption rate drastically, which is attributed to the hydrogen impermeability of TiN_x . Further investigations on the TiN_x films confirmed that hydrogen impermeability is considered to be controlled by the nitrogen content, i.e., volume ratios of titanium nitrides to metallic titanium, and that hydrogen permeates not through the domain consisting of titanium nitrides but only through the domain of metallic titanium, which serves as a hydrogen-diffusing path.

The authors also used *TiN*-coated titanium electrode prepared by cathodic arc ion-plating, and the dependence of hydrogen impermeability on the film thickness was investigated (Fig. 5). The observed anodic currents correspond to hydrogen uptake through the *TiN* film, and smaller anodic currents imply smaller hydrogen permeation through the surface film. Therefore, Fig. 5 clearly shows that hydrogen impermeability increases, as the film becomes thicker. The estimated diffusion coefficient of hydrogen through the *TiN* film was independent of the film thickness, about $1 \times 10^{-7} \text{ cm}^2 \text{ s}^{-1}$, which is one order larger than that for the gas-nitrided titanium sample. This might be caused by the columnar structure of the ion-plated *TiN* film. Therefore, the hydrogen impermeability of *TiN* films is controlled not only by the film thickness, but also by the morphological structure.

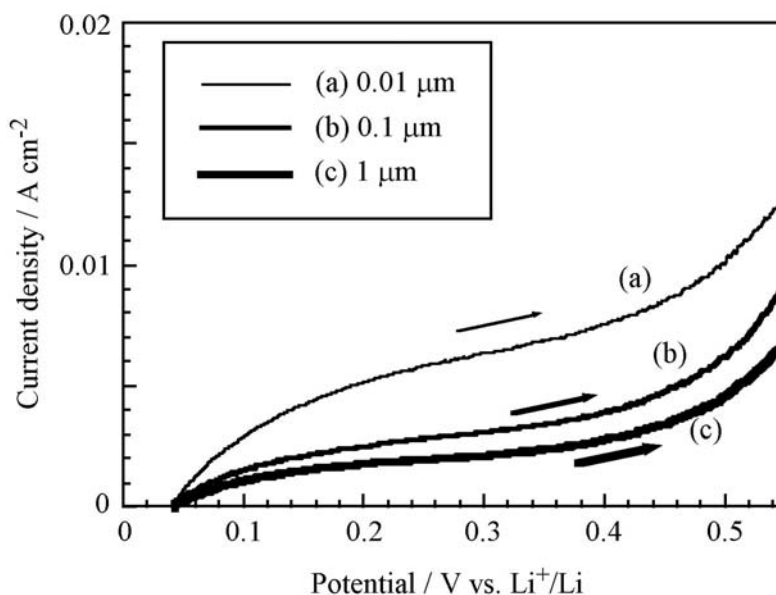


Figure 5. Typical linear sweep voltammograms for the surface nitrated electrodes prepared by cathodic arc ion-plating in LiCl-KCl-LiH (5.0 mol. % LiH added) melts at 723 K [23]. The thickness of the TiN layer is (a) $0.01 \mu\text{m}$, (b) $0.1 \mu\text{m}$ and (c) $1 \mu\text{m}$, respectively. Scan rate is 0.1 V sec^{-1} .

4. Alloy forming reactions

Transition metal (*TM*)-rare earth metal (*RE*) alloys are of great interest because of their excellent magnetic, hydrogen absorbing, hydrogen permeable, and catalytic properties. They can be formed by cathodic reduction of rare earth ions on a transition metal substrate in alkali metal chloride melts containing rare earth chlorides. The electrochemical alloy formation has been confirmed so far for the *Ni-Y* [29-31], *Ni-La* [32], *Ni-Nd* [33], *Ni-Dy* [34-37], *Ni-Sm* [38], *Ni-Ce* [39], *Ni-Pr* [40], *Ni-Yb* [41], *Fe-Nd* [33], *Fe-Dy* [42], *Co-Sm* [43], *Co-Gd* [44], *Pd-Y* [45], *Pd-La* [46], and *Pd-Ce* [47] systems. For example, *Ni-Y* intermetallic compounds are formed by cathodic reduction of *Y(III)* ion on a *Ni* electrode in LiCl-KCl-YCl_3 melts at 773 K [31]. Figure 6(a) shows the cross-sectional SEM image of the sample obtained by potentiostatic electrolysis at 0.5 V (vs. Li^+/Li) for 1 hour. The alloy layer was found to consist of almost uniform Ni_2Y phase according to XRD analysis. Furthermore, the growth rate of the single Ni_2Y phase was extremely large compared to the conventional solid state diffusion, e.g., the diffusion coefficient of *Y* in Ni_2Y was estimated to be $2.84(-0.40) \times 10^{-8} \text{ cm}^2 \text{ s}^{-1}$ at 773 K [30]. Electrochemical parameters (potential, current density etc.) strongly affect the growth

rate of the single Ni_2Y layer, which proceeds by the inter-diffusion of Ni and Y after electrodepositing Y on Ni . Since this phenomenon was difficult to explain by ordinary concepts of electrodeposition followed by solid phase diffusion, the phenomenon was called “electrochemical implantation” [48-49]. The rapid growth of a certain single alloy phase might be explained by the formation of microscopic cracks and/or grain boundaries that serve as the fast diffusion paths. Concerning the Ni - Y system, it was speculated by the molecular dynamics simulation the rapid growth is mainly due to the high-rate self-diffusion in and near the grain boundaries [50].

On the other hand, anodic polarization of the Ni_2RE alloy results in an interesting phenomenon; that is, rapid selective dissolution of RE leads to the transformation to another Ni - RE alloy or Ni , often accompanied by porous structure formation. Fig. 6(b) shows the electrode after the anodic dissolution of Y from Ni_2Y by anodic sweep electrolysis [31].

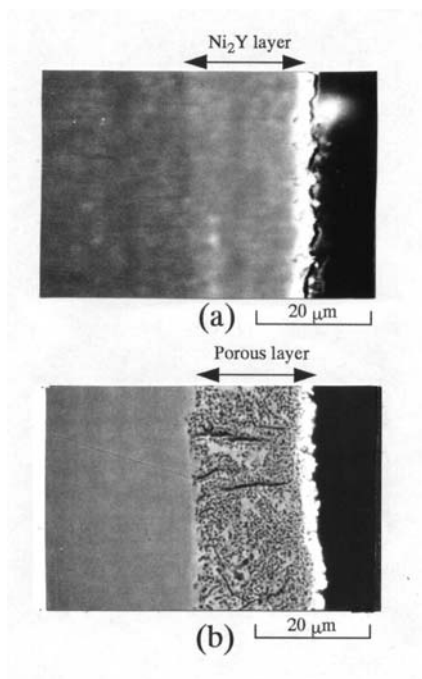


Figure 6. Cross-sectional SEM images of Ni-Y film formed by: (a) potentiostatic electrolysis at 0.50 V for 1 hour and (b) applying anodic potential sweep from 0.5 V to 2.25 V at a rate of 1 mV sec⁻¹ in LiCl-KCl-YCl₃ (0.17 mol. %) at 773 K.

The obtained porous layer was identified as pure Ni in this case. It has also been shown that the phase can be changed to Ni_3Y or Ni_5Y depending on the applied potential

value. The phase and structure changes can be accomplished even within a few minutes. Such a phenomenon has been called by the authors and co-workers “electrochemical displantation”. This phenomenon was also confirmed for the *Ni-Dy* system [34, 42]. *Ni₂Dy* alloy formed by “electrochemical implantation” was also transformed to porous *Ni-Dy* alloy or porous *Ni* by rapid anodic dissolution of *Dy*. The pore sizes were changed depending on the applied potential. In the newest results on this system, however, the rapid anodic dissolution of *Dy* was not observed on the annealed *Ni₂Dy* film. Therefore, it is believed that the microscopic cracks and/or grain boundaries introduced by “electrochemical implantation” are responsible for the rapid anodic dissolution of *Dy*, and that the annealing procedure leads to their decrement. The porous structure formation might be due to the volume change accompanied by the rapid transformation, whose clarification would need further investigations.

The combination of electrochemical implantation and displantation seems to have the potential of forming various transition metal-rare earth metal alloys at a high rate and with simultaneous control of the phases and microstructures.

5. Non-conventional electrochemical reactions

Recently, the authors and co-workers have been challenging to invent non-conventional electrochemical reactions in success. Some results will be described in the following sections, which includes examples related not only to the production of highly functionalized materials but also to useful industrial processes.

5.1. Direct electrolytic reduction of solid *SiO₂* to produce *Si*

SiO₂ is a well-known insulator and it is conventionally reduced to silicon by carbothermal reduction [51]. The electrochemical deoxidation of *SiO₂* has never been tried due to its high insulation and lack of appropriate techniques. Very recently, the authors and co-workers have reported a new electrochemical method for removing oxygen from solid *SiO₂* in a molten *CaCl₂* electrolyte [52]. In this method, the concept of “contacting electrode” has been newly introduced, in which a metal wire supplies electrons to the insulating solid *SiO₂*. Figs. 7a, b and c show photographs of the specimens obtained by potentiostatic electrolysis of the contacting electrode at 0.7 V. It is seen that even a short time (1 minute) was enough for the reaction to proceed, and the reaction zone spread out radially from the contacting point as the time passed. From the cross-sectional SEM images of the specimen (Figs. 7d and e), the reaction is also found to proceed inwardly. The core *SiO₂* is covered with the reduced silicon layer (100-200 μm thick) which consists of silicon columns with a diameter of 5-10 μm (Fig. 7e). By using EPMA, the composition of columns was found to be 90 at. % *Si* and 8 at. % *O*. These results

demonstrate that the reduction of insulating SiO_2 to silicon occurs electrochemically. In case no washing treatment was conducted after the electrolysis, filling of molten salt at the formed silicon layer was confirmed. Therefore, the observed fast reduction might be explained by the following scheme: firstly, the space is formed by the reduction of SiO_2 due to the decrease of molar volume from SiO_2 ($22.6 \text{ cm}^3 \text{ mol}^{-1}$) to Si ($12.1 \text{ cm}^3 \text{ mol}^{-1}$). Then, molten salt soaks into the space between the silicon columns. Since the formed silicon becomes new conduction path, the fresh reaction interface is produced continuously.

The most remarkable feature of this method is that the reduction can be done at any point by using the contacting electrode. This method is expected to be applicable to other various kinds of insulating materials, which have been believed as electrochemically inert.

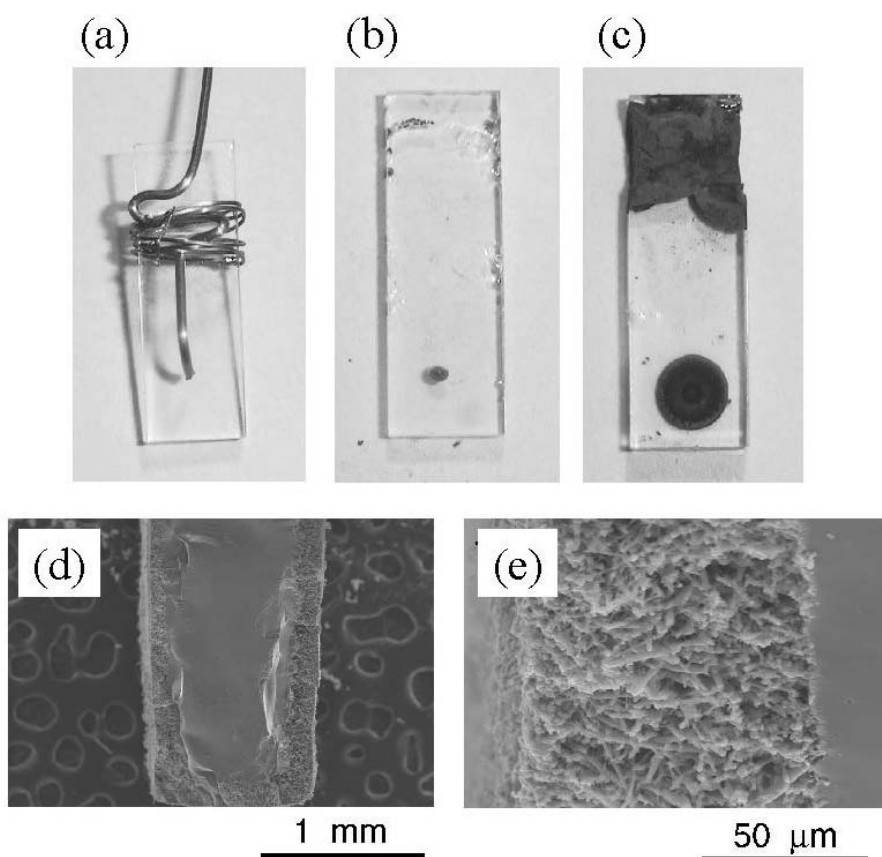


Figure 7. SEM images of SiO_2 point-contacting electrodes before (a) and after potentiostatic electrolysis at 0.7 V (vs. Li^+/Li) for 1 minute (b) and for 15 minutes (c) in molten CaCl_2 at 1173 K. Cross-sectional SEM images at low (d) and high (e) magnification of the specimen obtained at 1.0 V for 1 hour show the reduced Si layer consists of Si columns.

5.2. Discharge electrolysis

In molten chlorides, it is possible to conduct discharge electrolysis without using complicated apparatus: the electrodes are located in the electrolytic bath, but even in the case when one electrode is outside the bath, stationary discharge makes electrolysis possible under appropriate conditions. It has been already confirmed that a new type of stationary cathode discharge electrolysis is possible in molten salts at atmospheric pressure with a simple apparatus. For example, in the case of melts containing Ag^+ ion, fine spherical particles of Ag were obtained from the melt after the cathode discharge electrolysis [53]. It has also been confirmed that fine particles of Ni , Fe and carbon can be obtained in a similar way [54-55].

Recently, it has been investigated the possibility of the anode discharge electrolysis to produce fine particles of metal compounds. As an example, anode discharge electrolysis was conducted with titanium anode and $LiCl-KCl-CaO$ melts. After that, titanium oxide particles with sizes less than 150 nm were obtained as shown in Fig. 8 [56]. These particles are supposed to be formed by the reaction of $Ti(II)$, which is emitted from the anode to the melt, with oxide ion in the melt. The particle size is strongly affected by electrolytic conditions such as total flow of electricity, CaO concentration, bath temperature and volume. When iron, nickel or copper wire was used as the anode, their oxide particles were obtained [57].

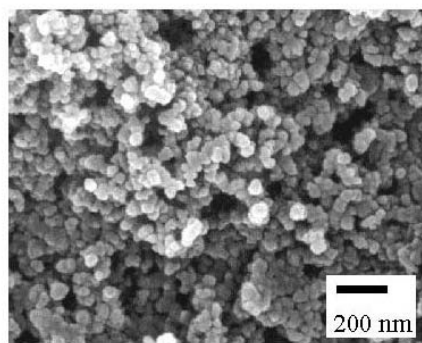


Figure 8. SEM image of the particles formed by anode discharge electrolysis of the $LiCl-KCl-CaO$ (0.2 mol. %) melt at 723 K. The anode was a titanium wire, the cathode was an aluminum plate, current - 800 mA, total flow of electricity - 100 C and bath volume - 0.06 dm³.

Moreover, by similar anode discharge electrolysis, metal sulfide particles were also obtained when using the metal anode and *LiCl-KCl-KSCN* melts [58]. This result suggests that this discharge method is expected to be a potential method for the production of fine metal compound particles of various kinds.

5.3. Electrochemical plantation on ceramics

A new electrochemical technique to form *Zr* metal and *Zr-Al* alloy films on ceramics has been successfully developed [59]. The outline of this method is shown in Fig.9. *Zr* metal is electrodeposited on a working electrode contacting with a ceramic plate. The metal then grows slowly along the ceramic surface almost two-dimensionally. It is revealed that the most important condition to ensure two-dimensional film growth is to form dendritic deposit on the working electrode at the beginning. This process will have a possibility to be developed to a new ceramic coating technique. For instance, this process can be combined with the nitriding method described above to obtain *Zr-N* coating on alumina.

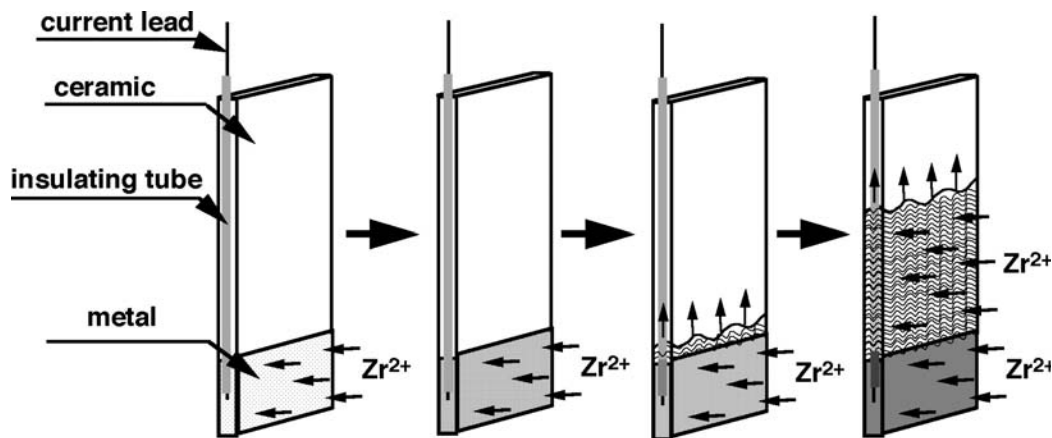


Figure 9. Insulating tube.

5.4. Electrolytic synthesis of NH_3

Most recently, the authors and co-workers have succeeded to synthesize ammonia under atmospheric pressure by utilizing similar electrochemical reaction of N^{3-}

represented in section 2. The principle is shown in Fig. 10 [60]. The anode is a hydrogen gas electrode having a porous structure or a hydrogen permeable membrane. On the anode, N^{3-} is oxidized and it reacts with hydrogen gas to produce ammonia according to reaction (5):

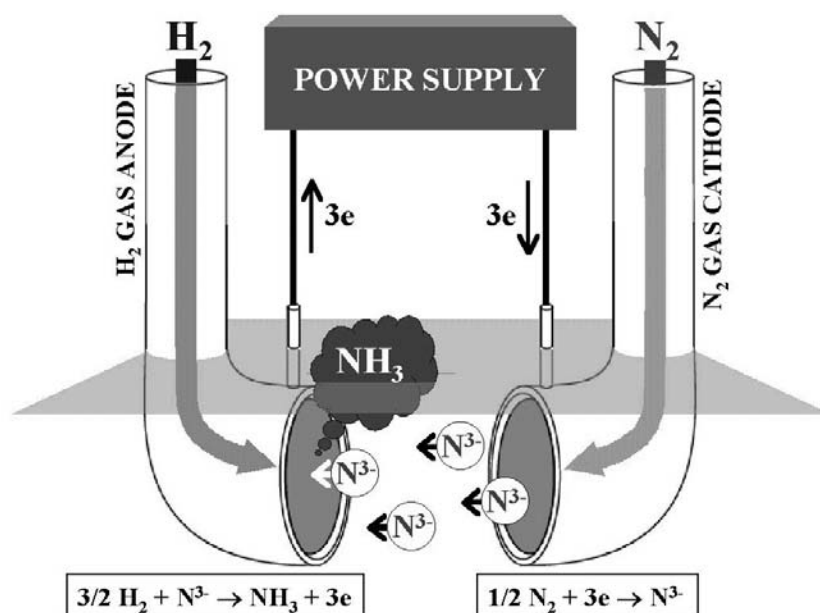


Figure 10. Schematic illustration of the electrolytic synthesis of ammonia in molten salts.

The N_2 gas cathode made of porous Ni is used, which continuously supplies N^{3-} by the reduction of nitrogen gas. It has been confirmed that ammonia is synthesized with an electrolysis voltage of about 0.3 V. The current efficiency of the process is more than 72 %, which was estimated by IR spectroscopy and pH titration with HCl solution.

From the rough cost evaluation, this novel method has a potential of applying to small-scale manufacturing of ammonia, for example, for the on-site use for the selective catalytic reduction of NO_x . Furthermore, it might become an alternative method of the Haber-Bosch process by improving the structure of the gas electrodes and optimizing the electrolysis conditions.

6. Conclusions

As described above, the authors and co-workers have investigated novel electrochemical reactions in molten salts, and found that they can be applied to produce various highly functionalized materials. The electrochemical methods utilizing these reactions have many attractive possibilities both in scientific and technological fields, which might have further potentials in the upcoming environmentally harmonious society. However, there are still technical issues that impede their practical-use application, such as corrosion of cell components, heat balance of the cell, dendritic deposition etc. In order to overcome these problems, more intensive and systematic studies in scientific, technological and economical aspects are required.

References

1. K. Grjotheim, C. Krohn, M. Malinovsky, K. Matiasovsky and J. Thonstad, Aluminum Electrolysis, Aluminum-Verlag, Düsseldorf, 1977.
2. J. Thonstad, Advances in Molten Salt Chemistry, G. Mamantov, C.B. Mamantov, J. Braunstein (Editors), Elsevier, Amsterdam, 1987, vol. 6, p. 73.
3. M. Sørli and H. Hye, Cathodes in Aluminum Electrolysis, Second Edition, Aluminum-Verlag, Düsseldorf, 1994.
4. G.J. Kipouros and D.R. Sadoway, Advances in Molten Salt Chemistry, G. Mamantov, C.B. Mamantov, J. Braunstein (Editors), Elsevier, Amsterdam, 1987, vol. 6, p. 127.
5. D.G. Lovering, Molten Salt Technology, Plenum Press, New York, 1982.
6. A. Girginov, T.Z. Tzvetkoff and M. Bojinov, J. Appl. Electrochem., 25 (1995) 993.
7. B. Aladjov, A. Stoyanova, J.R. Selman and Y.P. Lin, Electrochemical Technology, N. Masuko, T. Osaka and Y. Ito (Editors), Kodansha, Tokyo, 1996, p. 301.
8. H. Numata, Hyomen Gijutsu (The Journal of the Surface Finishing Society of Japan, in Japanese), 49 (1998) 341.
9. T. Goto, M. Tada and Y. Ito, Electrochim. Acta, 39 (1994) 1107.
10. T. Nishikiori, T. Nohira, T. Goto and Y. Ito, Electrochem. Solid-State Lett., 2 (1999) 278.
11. T. Nishikiori, T. Nohira, T. Goto and Y. Ito, Electrochem. Solid-State Lett., 3 (2000) 552.
12. H. Ishigaki and Y. Ito, Proc. 29th Symposium on Molten Salt Chemistry, October 30-31, Fukuoka, Japan, 1997, p. 101.
13. T. Goto, R. Obata and Y. Ito, Electrochim. Acta, 45 (2000) 3367.
14. T. Goto, T. Iwaki and Y. Ito, Annual Report of Quantum Science and Engineering Center, 2001, vol. 3, p. 89.
15. H. Tsujimura, T. Goto and Y. Ito, Proc. 31st Symposium on Molten Salt

- Chemistry, November 11-12, Sendai, Japan, 1999, p. 29.
16. H. Tsujimura, T. Goto and Y. Ito, *Electrochim. Acta*, 47 (2002) 2725.
 17. M. Shimizu, T. Goto and Y. Ito, Proc. 29th Symposium on Molten Salt Chemistry, October 30-31, Fukuoka, Japan, 1997, p. 11.
 18. T. Goto and Y. Ito, Proc. Annual Meeting of The Electrochemical Society of Japan, April 4-6, Nagoya, Japan, 2000, p. 162.
 19. T. Goto, T. Saeki and Y. Ito, Annual Report of Quantum Science and Engineering Center, 2002, vol. 4, p. 86.
 20. H. Tsujimura, T. Goto and Y. Ito, *Electrochim. Acta*, 355 (2003) 315.
 21. T. Goto and Y. Ito, *Electrochim. Acta*, 43 (1998) 3379.
 22. T. Nishikiori, T. Nohira and Y. Ito, *J. Electrochem. Soc.*, 148(1) (2001) E38.
 23. T. Kasajima, T. Nishikiori, T. Nohira and Y. Ito, *Solid-State Lett.*, 6(5) (2003) E5.
 24. T. Kasajima, T. Nishikiori, T. Nohira and Y. Ito, *J. Electrochem. Soc.*, 355 (2003) 315.
 25. T. Nishikiori, T. Nohira and Y. Ito, *J. Electrochem. Soc.*, 148(3) (2001) E127.
 26. T. Nohira and Y. Ito, *J. Electrochem. Soc.*, 144 (1997) 2290.
 27. T. Nishikiori, T. Nohira and Y. Ito, *J. Electrochem. Soc.*, 148(1) (2001) E52.
 28. T. Nishikiori, T. Nohira and Y. Ito, *Thin Solid Films*, 408 (2002) 148.
 29. G. Xie, K. Ema and Y. Ito, *J. Appl. Electrochem.*, 23 (1993) 753.
 30. G. Xie, K. Ema and Y. Ito, *J. Appl. Electrochem.*, 24 (1994) 321.
 31. K. Tateiwa, M. Tada and Y. Ito, *Hyomen Gijutsu (The Journal of the Surface Finishing Society of Japan, in Japanese)*, 46 (1995) 673.
 32. T. Aisaka, M. Tada and Y. Ito, Proc. 47th Annual Meeting of The International Society of Electrochemistry, September 1-6, Veszprém & Balatonfüred, Hungary, 1996, L5e-1.
 33. T. Aisaka, M. Tada and Y. Ito, Proc. 28th Symposium on Molten Salt Chemistry, October 29-November 1, Kofu, Japan, 1996, p. 20.
 34. H. Konishi, T. Nohira and Y. Ito, *J. Electrochem. Soc.*, 148(7) (2001) C506.
 35. H. Konishi, T. Nohira and Y. Ito, *Electrochem. Solid-State Lett.*, 5(12) (2002) B37.
 36. H. Konishi, T. Nohira and Y. Ito, *Electrochim. Acta*, 48 (2003) 563.
 37. H. Konishi, T. Nishikiori, T. Nohira and Y. Ito, *Electrochim. Acta*, 48(2003) 1403.
 38. T. Iida, T. Nohira and Y. Ito, *Electrochim. Acta*, 46 (2001) 2537.
 39. T. Ohi, T. Nohira and Y. Ito, Proc. Annual Meeting of The Electrochemical Society of Japan, April 1-3, Kobe, Japan, 2001, p. 208.
 40. H. Kambara, T. Nohira and Y. Ito, Proc. 34th Symposium on Molten Salt Chemistry, November 21-22, Toyohashi, Japan, 2002, p. 77.
 41. T. Iida, T. Nohira and Y. Ito, *Electrochim. Acta*, 48 (2003) 1531.
 42. H. Konishi, T. Nohira and Y. Ito, *Electrochim. Acta*, 47 (2002) 3533.
 43. T. Iida, T. Nohira and Y. Ito, *Electrochim. Acta*, 48 (2003) 901.

44. T. Kubota, T. Iida, T. Nohira and Y. Ito, *Electrochim. Acta*, submitted.
45. E.O. Ahlgren, T. Nohira and Y. Ito, *J. Alloys Compds.*, submitted.
46. H. Qiao, T. Nohira and Y. Ito, *J. Alloys Compd.*, in press.
47. T. Nohira, H. Konishi, T. Iida, T. Ohi and Y. Ito, Annual Report of Quantum Science and Engineering Center, 2000, vol. 2, p. 92.
48. Y. Ito and T. Nohira, *Hyomen Gijutsu (The Journal of the Surface Finishing Society of Japan, in Japanese)*, 49 (1998) 336.
49. Y. Ito and T. Nohira, *Electrochim. Acta*, 45 (2000) 2611.
50. K. Hachiya and Y. Ito, *J. Alloys Compd.*, 279 (1998) 171.
51. W. Zulehner, *Ullmann's Encyclopedia of Industrial Chemistry*, 5th edition, B. Elvers, S. Hawkins, W. Russey and G. Schulz (Editors), VCH Verlagsgesellschaft, 1993, vol. A23, p. 721.
52. T. Nohira, K. Yasuda and Y. Ito, *Nature Materials*, 2 (2003) 397.; T. Nohira, K. Yasuda and Y. Ito, *Proc. Asian Conference on Electrochemistry 2002, Jeju Island, Korea, 2002*, p. 658.
53. H. Kawamura, K. Moritani and Y. Ito, *Plasmas and Ions*, 1 (1998) 29.
54. H. Kawamura, K. Moritani and Y. Ito, *J. Jpn. Soc. Powder and Powder Metallurgy*, 45 (1998) 1142.
55. H. Kawamura, K. Moritani and Y. Ito, *J. Appl. Electrochem.*, 30 (2000) 571.
56. T. Oishi, T. Goto and Y. Ito, *J. Appl. Electrochem.*, 32 (2002) 819.
57. T. Oishi, T. Goto and Y. Ito, *J. Electrochem. Soc.*, 149(11) (2002) D155.
58. T. Oishi, T. Goto and Y. Ito, *Electrochemistry*, 70(9) (2002) 697.
59. M. Kawase, M. Tada and Y. Ito, *Hyomen Gijutsu (The Journal of the Surface Finishing Society of Japan, in Japanese)*, 44 (1993) 5.
60. T. Murakami, T. Nishikiori, T. Nohira and Y. Ito, *J. Am. Chem. Soc.*, 125 (2003) 334.